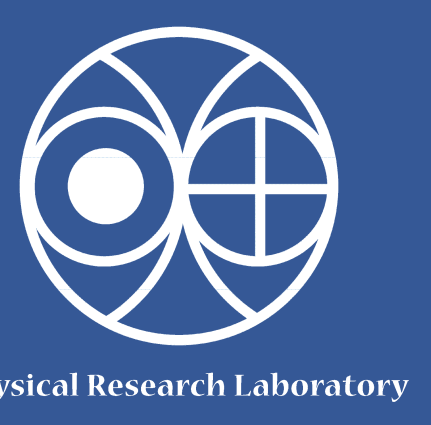


Goldstone modes, bifurcations and interaction induced instability of dark solitons in segregated Bose-Einstein condensates at finite temperature

Arko Roy¹, S. Gautam², and D. Angom¹

¹Physical Research Laboratory, Ahmedabad - 380 009, Gujarat, India
²UNESP - Universidade Estadual Paulista, 01.140-070 São Paulo, Brazil



Introduction

Outline:

- Emergence of the third Goldstone mode in binary condensates at phase-separation for density profiles where one component is surrounded on both sides by the other component.
- At higher interspecies interaction, the third Goldstone mode persists for the above case. This does not happen in symmetry-broken density profiles where one species is entirely to the left and the other is entirely to the right.
- We use Hartree-Fock-Bogoliubov theory with Popov approximation to examine the mode evolution at $T \neq 0$ and demonstrate the existence of mode bifurcation near the critical temperature.
- The Kohn mode exhibits deviation from the natural frequency at finite temperatures after the phase separation.

Theory

- For a quasi-1D system (cigar shaped condensate) the trapping potential $V = (1/2)m(\omega_x^2 x^2 + \omega_y^2 y^2 + \omega_z^2 z^2)$, the trapping frequencies should satisfy the condition $\omega_x = \omega_y = \omega_\perp \gg \omega_z$.
- Grand-canonical Hamiltonian, in the second quantized form, describing the mixture of two interacting BECs is given by

$$H = \sum_{k=1,2} \int dz \hat{\Psi}_k^\dagger(z, t) \left[-\frac{\hbar^2}{2m_k} \frac{\partial^2}{\partial z^2} + V_k(z) - \mu_k + \frac{U_{kk}}{2} \hat{\Psi}_k^\dagger(z, t) \hat{\Psi}_k(z, t) \right] \hat{\Psi}_k(z, t) + U_{12} \int dz \hat{\Psi}_1^\dagger(z, t) \hat{\Psi}_1(z, t) \hat{\Psi}_2(z, t) \hat{\Psi}_2^\dagger(z, t),$$

The strength of intra- and inter-species interactions are $U_{kk} = (a_{kk}\lambda)/m_k$ and $U_{12} = (a_{12}\lambda)/(2m_{12})$, respectively, where $\lambda = (\omega_\perp/\omega_z) \gg 1$ is the anisotropy parameter.

- Equation of motion of the Bose field operators is

$$i\hbar \frac{\partial}{\partial t} \begin{pmatrix} \hat{\Psi}_1 \\ \hat{\Psi}_2 \end{pmatrix} = \begin{pmatrix} \hat{h}_1 + U_{11} \hat{\Psi}_1^\dagger \hat{\Psi}_1 & U_{12} \hat{\Psi}_2^\dagger \hat{\Psi}_1 \\ U_{12} \hat{\Psi}_1^\dagger \hat{\Psi}_2 & \hat{h}_2 + U_{22} \hat{\Psi}_2^\dagger \hat{\Psi}_2 \end{pmatrix} \begin{pmatrix} \hat{\Psi}_1 \\ \hat{\Psi}_2 \end{pmatrix}$$

where $\hat{h}_k = (-\hbar^2/2m_k)\partial^2/\partial z^2 + V_k(z) - \mu_k$. We define $\hat{\Psi}(z, t) = \hat{\Phi}(z) + \hat{\Psi}(z, t)$, where $\hat{\Phi}(z)$ is a c -field and represents the condensate, and $\hat{\Psi}(z, t)$ is the fluctuation part.

$$\begin{pmatrix} \hat{\Psi}_1 \\ \hat{\Psi}_2 \end{pmatrix} = \begin{pmatrix} \hat{\phi}_1 \\ \hat{\phi}_2 \end{pmatrix} + \begin{pmatrix} \hat{\psi}_1 \\ \hat{\psi}_2 \end{pmatrix},$$

For a TBEC, ϕ_k s are the stationary solutions of the coupled generalized GP equations, with time-independent HFB-Popov approximation, given by

$$\hat{h}_1 \phi_1 + U_{11} [n_{c1} + 2\tilde{n}_1] \phi_1 + U_{12} n_2 \phi_1 = 0, \\ \hat{h}_2 \phi_2 + U_{22} [n_{c2} + 2\tilde{n}_2] \phi_2 + U_{12} n_1 \phi_2 = 0,$$

where, $n_{ck}(z) \equiv |\phi_k(z)|^2$, $\tilde{n}_k(z) \equiv \langle \hat{\psi}_k^\dagger(z, t) \hat{\psi}_k(z, t) \rangle$, and $n_k(z) = n_{ck}(z) + \tilde{n}_k(z)$ are the local condensate, non-condensate, and total density, respectively.

Hartree-Fock-Bogoliubov-Popov approximation

Using Bogoliubov transformation

$$\hat{\psi}_k(z, t) = \sum_j \left[u_{kj}(z) \hat{\alpha}_j(z) e^{-iE_j t} - v_{kj}^*(z) \hat{\alpha}_j^\dagger(z) e^{iE_j t} \right],$$

where, $\hat{\alpha}_j$ ($\hat{\alpha}_j^\dagger$) are the quasi-particle annihilation (creation) operators.

- Bogoliubov-de Gennes equations (BdG) for TBEC

$$\hat{L}_1 u_{1j} - U_{11} \phi_1^* v_{1j} + U_{12} \phi_1 (\phi_2^* u_{2j} - \phi_2 v_{2j}) = E_j u_{1j}, \\ \hat{L}_1 v_{1j} + U_{11} \phi_1 u_{1j} - U_{12} \phi_1^* (\phi_2 v_{2j} - \phi_2^* u_{2j}) = E_j v_{1j}, \\ \hat{L}_2 u_{2j} - U_{22} \phi_2^* v_{2j} + U_{12} \phi_2 (\phi_1^* u_{1j} - \phi_1 v_{1j}) = E_j u_{2j}, \\ \hat{L}_2 v_{2j} + U_{22} \phi_2 u_{2j} - U_{12} \phi_2^* (\phi_1 v_{1j} - \phi_1^* u_{1j}) = E_j v_{2j},$$

where $\hat{L}_1 = (\hat{h}_1 + 2U_{11}n_1 + U_{12}n_2)$, $\hat{L}_2 = (\hat{h}_2 + 2U_{22}n_2 + U_{12}n_1)$ and $\hat{L}_k = -\hat{L}_k$. To solve, we consider

$$u_{ij} = \sum_{i=0}^N p_{ij} \xi_i, \quad v_{ij} = \sum_{i=0}^N q_{ij} \xi_i, \\ u_{2j} = \sum_{i=0}^N r_{ij} \xi_i, \quad v_{2j} = \sum_{i=0}^N s_{ij} \xi_i,$$

where ξ_i is the i th harmonic oscillator eigenstate and p_{ij} , q_{ij} , r_{ij} and s_{ij} are the coefficients of linear combination.

- The number density \tilde{n}_k of the non-condensate atoms is

$$\tilde{n}_k = \sum_j \{ |u_{kj}|^2 + |v_{kj}|^2 \} N_0(E_j) + |v_{kj}|^2,$$

where $\langle \hat{\alpha}_j^\dagger \hat{\alpha}_j \rangle = (e^{\beta E_j} - 1)^{-1} \equiv N_0(E_j)$ is the Bose factor of the quasi-particle state with real and positive energy E_j .

It should be emphasized that, when $T \rightarrow 0$, $N_0(E_j)$'s vanishes. The non-condensate density is then reduced to

$$\tilde{n}_k = \sum_j |v_{kj}|^2.$$

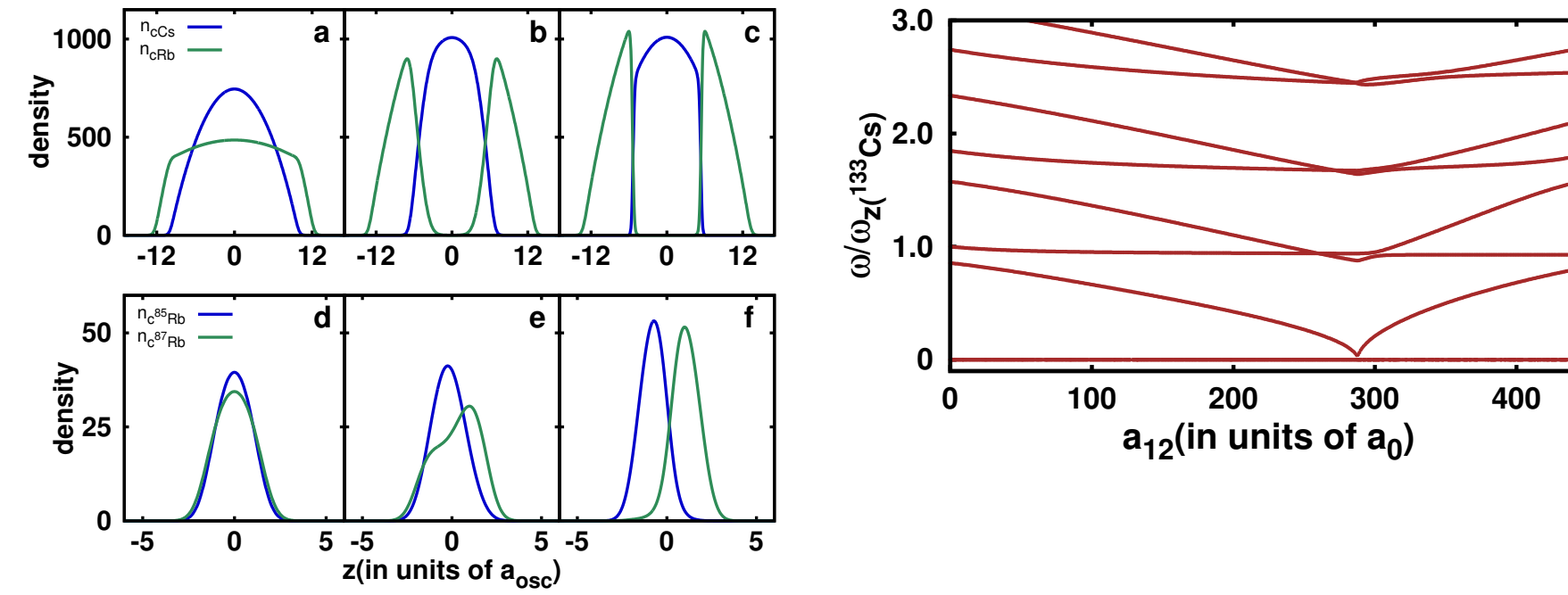
Thus, at zero temperature we need to solve the equations self-consistently as the quantum depletion term $|v_{kj}|^2$ in the above equation is non-zero.

Numerical Scheme

- For the $T = 0$ studies we solve the pair of coupled GP equations by neglecting the non-condensate density ($\tilde{n}_k = 0$) using Crank-Nicholson method adapted for binary condensates.
- Using the stationary ground state wave function of the TBEC, we cast the BdG equations as a matrix eigenvalue equation in the basis of the trapping potential.
- The matrix is then diagonalized using the LAPACK routine `zgeev` to find the quasi-particle energies and amplitudes, E_j , and u_k 's and v_k 's, respectively. These u_k 's and v_k 's along with E_j are used to get the initial estimate of \tilde{n}_k .
- Using this updated value of \tilde{n}_k , the ground state wave function of TBEC ϕ_k and chemical potential μ_k are again re-calculated. This procedure is repeated till the solutions reach desired convergence.
- In general, the convergence is not smooth and we encounter severe oscillations very frequently. To damp the oscillations and accelerate convergence we employ successive over (under) relaxation technique for updating the condensate (non-condensate) densities.

Results at $T = 0$

Mode evolution & density profiles of trapped TBEC

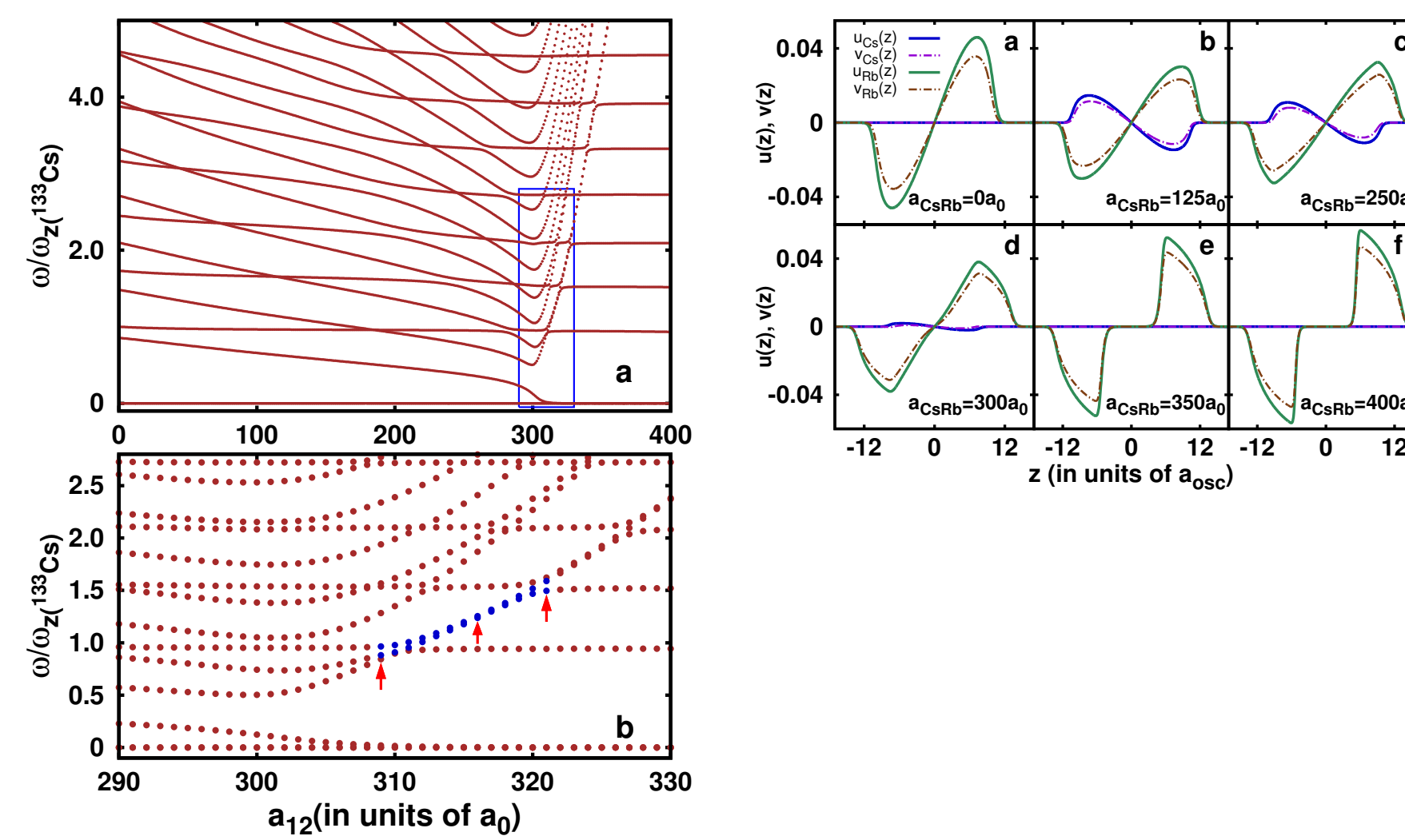


First panel – Miscible to sandwich type density profile with $a_{\text{CsRb}} = \{200a_0, 310a_0, 420a_0\}$ respectively.

Second panel – Miscible to side-by-side density profile with $a_{\text{RbRb}} = \{100a_0, 290a_0, 400a_0\}$ respectively.

Right figure – Low-lying modes of ^{85}Rb - ^{87}Rb . At phase separation the structure of the density profiles is side-by-side and one of the modes goes soft.

Trapping frequencies: $\omega_z(\text{Rb}) = 2\pi \times 3.89\text{Hz}$ and $\omega_z(\text{Cs}) = 2\pi \times 4.55\text{Hz}$. $\omega_\perp(\text{Cs}) = 2\pi \times 40.2\text{Hz}$ and $\omega_\perp(\text{Rb}) = 2\pi \times 32.2\text{Hz}$

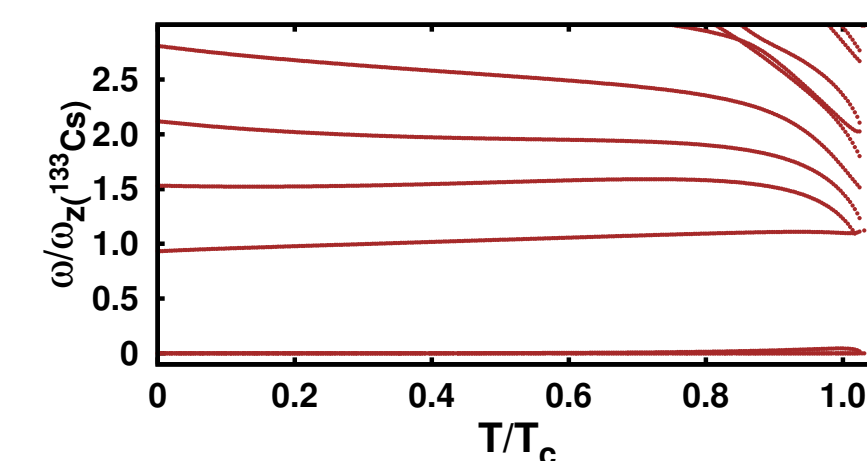


Left figure – Evolution of the low-lying modes in the domain $0 \leq a_{\text{CsRb}} \leq 400a_0$ for $N_{\text{Rb}} = N_{\text{Cs}} = 10^4$. Third Goldstone mode emerges.

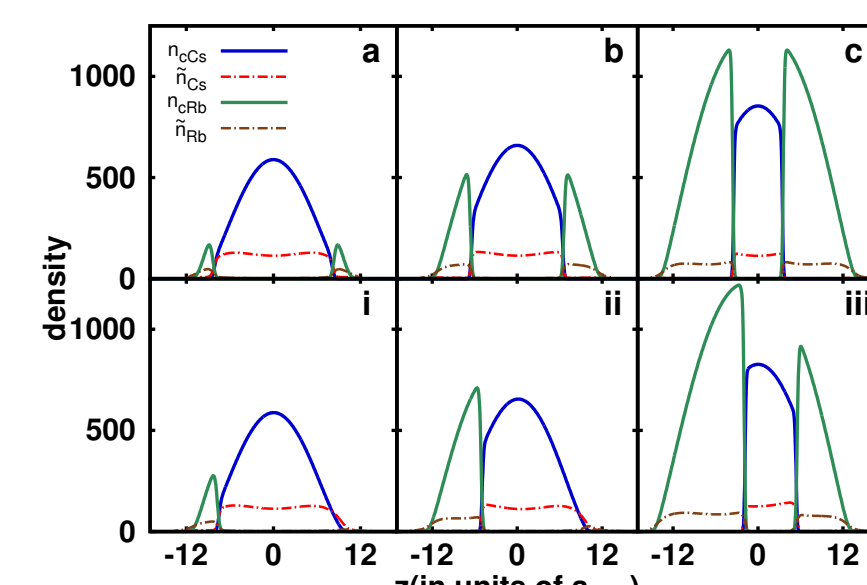
Right figure – Evolution of quasi-particle amplitude corresponding to the Rb Kohn mode as a_{CsRb} is increased from 0 to $400a_0$.

Results at $T \neq 0$

Mode evolution & density profiles of trapped TBEC

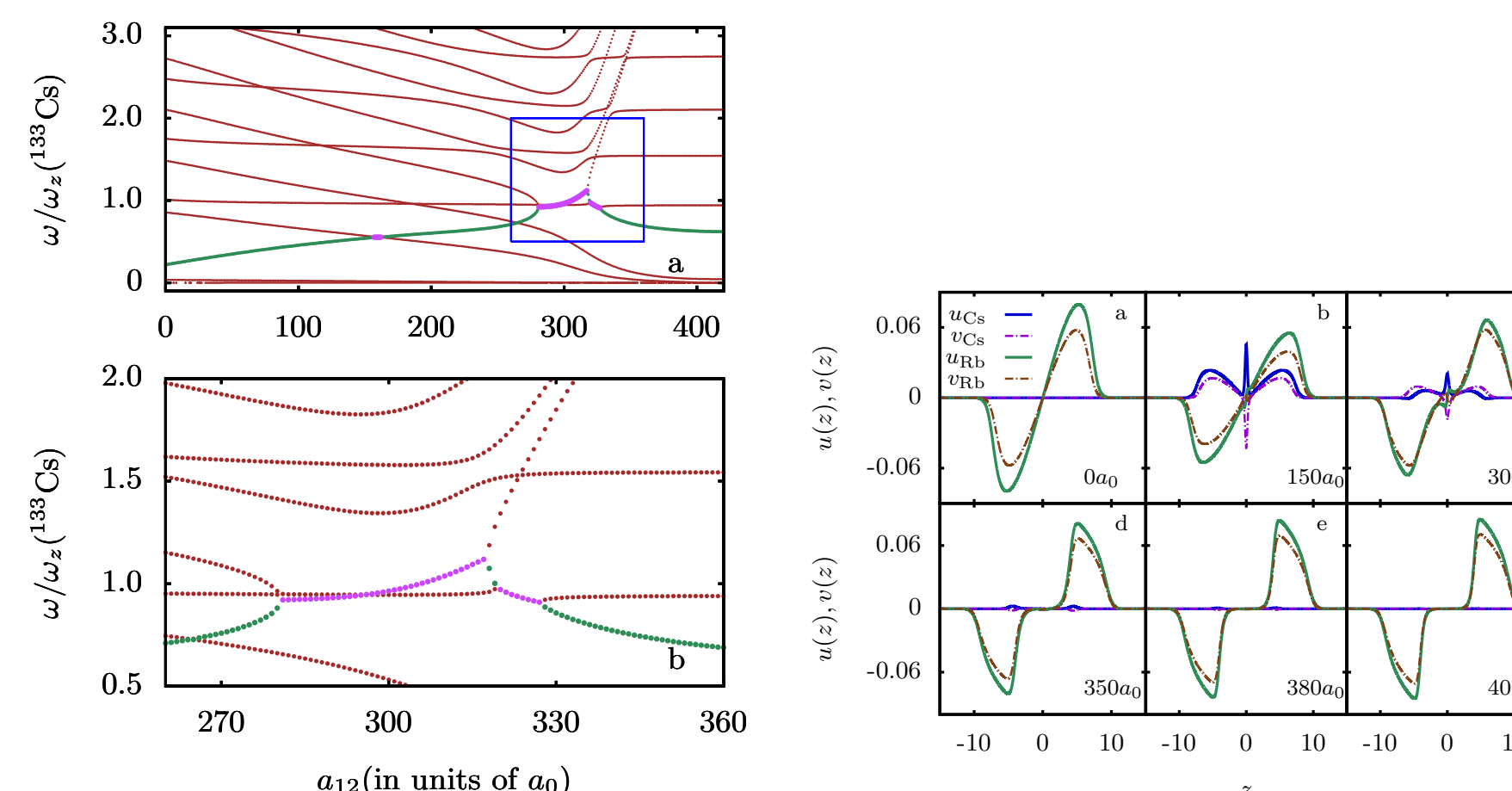


Frequencies (ω_j) of the low-lying modes at $T/T_c \neq 0$ with $N = 10^3$. Evolution of the modes indicates bifurcations at $T/T_c \approx 1$.



Profiles correspond to $N_{\text{Rb}} = 840(N_{\text{Cs}} = 8570)$, $N_{\text{Rb}} = 3680(N_{\text{Cs}} = 8510)$, and $N_{\text{Rb}} = 15100(N_{\text{Cs}} = 6470)$, at $T = 25nK$.

Results of TBEC with soliton at $T = 0$

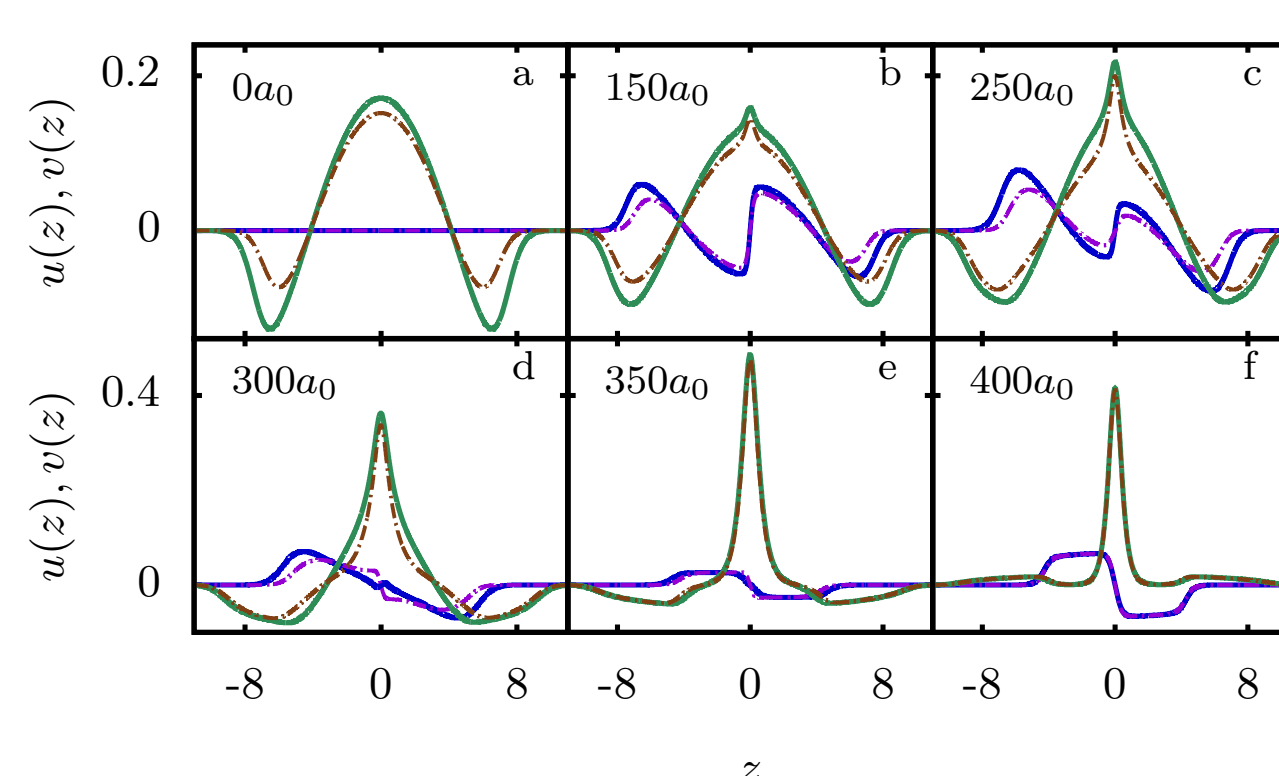


Left figure – Evolution of the low-lying modes in the domain $0 \leq a_{\text{CsRb}} \leq 420a_0$ for $N_{\text{Rb}} = N_{\text{Cs}} = 10^4$. Third and fourth Goldstone mode emerges.

Emergence of fourth Goldstone mode :

Right figure – Evolution of quasi-particle amplitude corresponding to the Rb Kohn mode as a_{CsRb} is increased from 0 to $420a_0$.

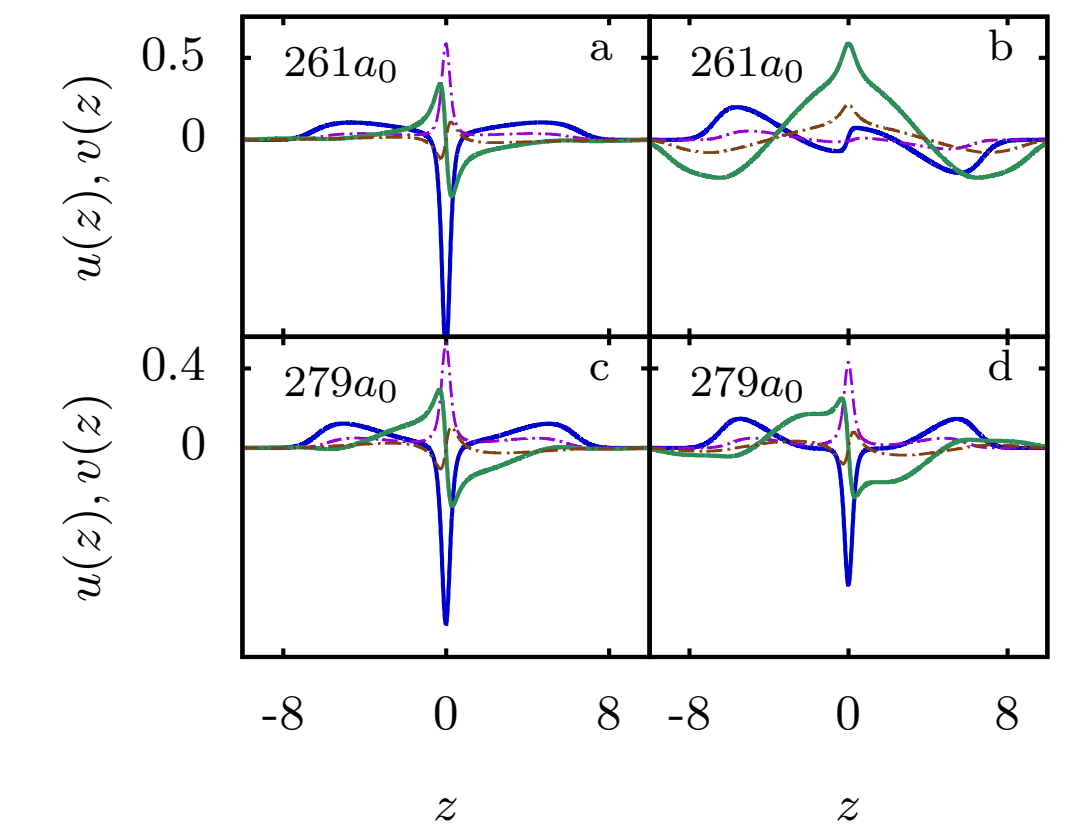
Trapping frequencies: $\omega_z(\text{Rb}) = 2\pi \times 3.89\text{Hz}$ and $\omega_z(\text{Cs}) = 2\pi \times 4.55\text{Hz}$. $\omega_\perp(\text{Cs}) = 30\omega_z(\text{Cs})\text{Hz}$ and $\omega_\perp(\text{Rb}) = 30\omega_z(\text{Rb})\text{Hz}$.



Evolution of quasi-particle amplitude corresponding to the fourth excited mode as a_{CsRb} is increased from 0 to $420a_0$.

Nature of mode collisions

- Green dots – anomalous modes.
- Purple dots – complex modes.
- Several instances of avoided crossings and mode collision are evident.
- Salient features:
 - Mode collision occurs when the anomalous mode collides with an excited state.
 - The modes either cross each other or undergo bifurcation giving rise to complex eigenmodes.

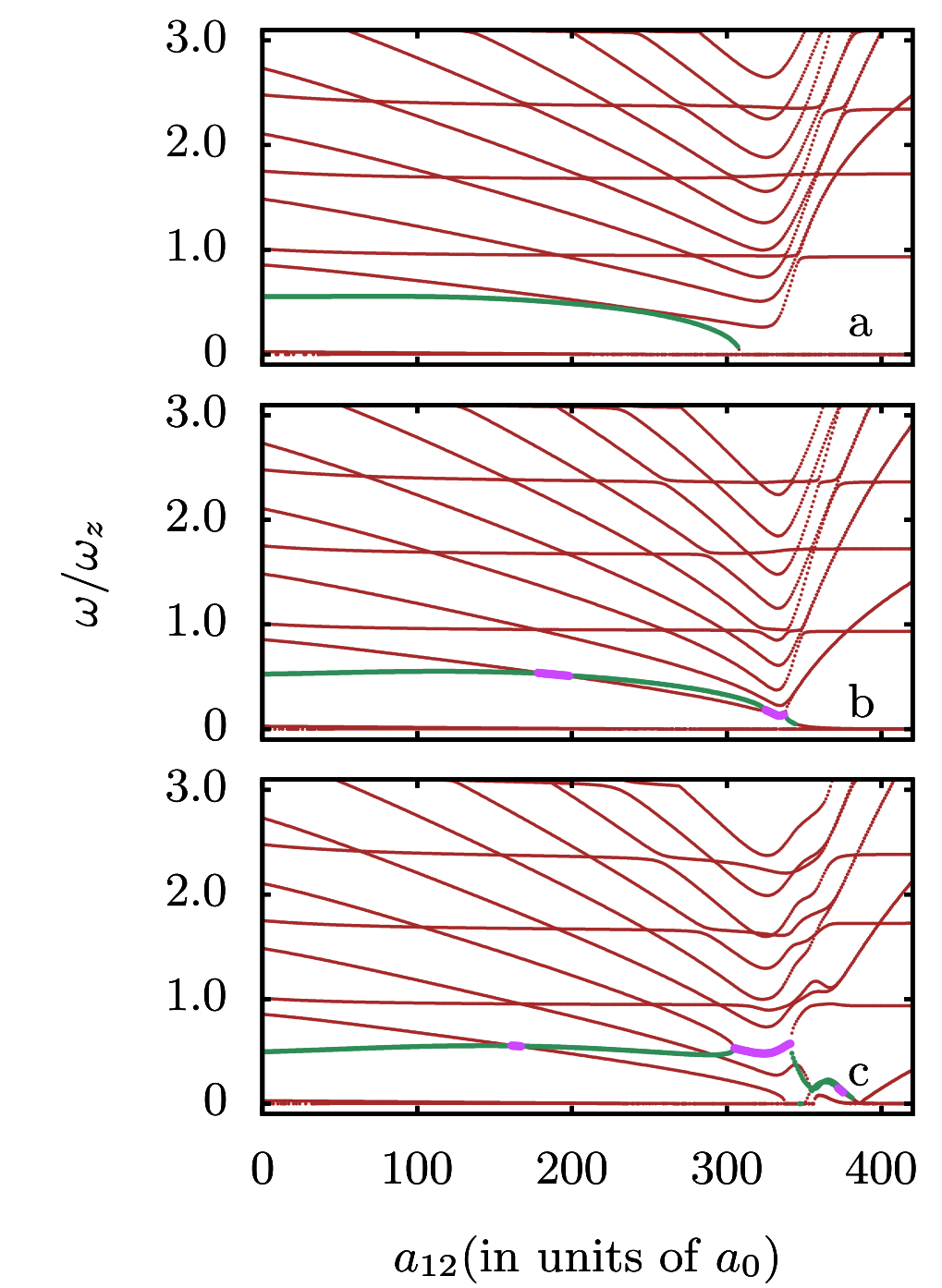


(a-b) Quasi-particle amplitude corresponding to the anomalous and fourth excited mode respectively, for $a_{\text{CsRb}} = 261a_0$.

(c-d) Quasi-particle amplitude corresponding to the anomalous and sixth excited mode respectively, for $a_{\text{CsRb}} = 279a_0$. These two modes after colliding gives rise to complex eigenfrequencies, which makes the system oscillatory unstable.

Different mass ratios

Interplay of mass difference and intra-species scattering length:



The evolution of the low-lying modes of the TBEC with soliton for different mass ratios as a function of the inter-species scattering length a_{12} in the domain $0 \leq a_{12} \leq 420a_0$. The masses of the first and second species in each of the panels correspond to (a) 95 and 87, (b) 100 and 87, and (c) 105 and 87 amu, respectively for $N_i = 10^3$. The intra-species scattering lengths of the first and second species are $a_{11} = 280a_0$ and $a_{22} = 100a_0$, respectively. Shown here is only the real part of ω/ω_z .

Characteristic Features:

- In Fig. (a) with $m_1 = 95$, the anomalous mode goes soft at phase separation and becomes the third Goldstone mode of the system. In addition, there are no mode collisions involving the anomalous mode.
- In Fig. (b) with $m_1 = 100$ two major changes in the mode evolution are evident: there is an additional mode below the Kohn mode; and anomalous mode collides with the second excited mode twice at $a_{12} \approx 180a_0$ and $320a_0$. The emergence of a bifurcation is evident in the second mode collision at $a_{12} \approx 320a_0$.
- In Fig. (c), the trend in the mode collision for $m_1 = 105$ bear close resemblance to the ^{87}Rb - ^{133}Cs mixture. In this case, the bifurcation arising from the collision between the anomalous and sixth excited mode is quite evident.

- Soliton induced change in the density profiles when the atomic masses of the two species differ widely. Based on a series of computations, we find an enhancement in the mass ratio at which the heavier species, with higher scattering length, occupies the central position at phase separation.

Conclusions

- In TBEC with dark soliton at $z = 0$ with strong interspecies interaction, we observe four Goldstone modes.
- TBECs with soliton in one of the components oscillate while interacting even at zero temperature. This is due to the non-zero density of the species without the soliton within the notch of the dark soliton.

References

- [1] A. Roy, S. Gautam and D. Angom, Phys. Rev. A **89**, 013617, (2014).
- [2] S. Gautam and D. Angom, J. Phys. B **43**, 095302, (2010).
- [3] S. Gautam and D. Angom, J. Phys. B **44**, 025302, (2011).
- [4] Simula et al, Comp. Phys. Comm. **142**, 396, (2001).
- [5] McCarron et al, Phys. Rev. A **84**, 011603, (2011).
- [6] Middelkamp et al, Phys. Rev. A **81**, 053618, (2010).
- [7] J. Dziarmaga and K. Sacha, Phys. Rev. A **66**, 043620, (2002).
- [8] A. Griffin, Phys. Rev. B **53**, 9341, (1996).